CHAPTER III
IMPROVEMENT OF ELECTROMECHANICAL PROPERTIES OF GELATIN HYDROGELS BY BLENDING WITH NANOWIRE-POLYPYRROLE: EFFECT OF ELECTRIC FIELD AND TEMPERATURE

3.1 Abstract

Nanowire-Polypyrrole/gelatin hydrogels were fabricated by the dispersion of nanowire-polypyrrole into the gelatin aqueous solution followed by the solvent casting. The electromechanical properties, thermal properties and deflection of pure gelatin hydrogel and nanowire-polypyrrole/gelatin hydrogels were studied as functions of temperature, frequency, and electric field strength. The 0.01, 0.1, 0.5, 1 %v/v nanowire-polypyrrole/gelatin hydrogels and pure gelatin hydrogel possess storage modulus sensitivity values of 0.75, 1.04, 0.88, 0.99 and 0.46, respectively, at the electric field strength of 800 V/mm. The effect of temperature on the electromechanical properties of the pure gelatin hydrogel and nanowire-polypyrrole/gelatin hydrogels were investigated between 30 °C and 80 °C; there are three regimes for the storage modulus behavior. In the deflection testing in the cantilever fixture, the dielectrophoresis force was determined and found to increase monotonically with electric field strength. The pure gelatin hydrogel possesses the highest deflection angle and dieletrophoresis force at the electric field strength of 800 V/mm relative to those of the nanowire-polypyrrole/gelatin hydrogels.

Keywords: Biopolymer; Gelatin; Hydrogels; Conducting polymers; Actuator

3.2 Introduction

The exchange of electrical energy and mechanical energy has been of scientific and technological interest for many decades. Electroactive polymers (EAPs) offer promising and novel characteristics such as lightweight, high energy density, and high flexibility. They are also candidates for muscle–like actuator materials. Some of the currently available materials are ionic polymer-metal composites (IPMC) (Shahinpoor *et al.*, 1998), gel-polymers (Calvert *et al.*, 1998), conductive polymers (Macdiarmid *et al.*, 1985), electric field activated EAPs such as electron irradiated (PVDF TrFE) (Zhang *et al.*, 1998), dielectric elastomers (Perlin *et al.*, 1998), electrostrictive polymer artificial muscle (EPAM) (Kim *et al.*, 2006; Bar cohen *et al.*, 2001), and electrorheological fluids (Koyama *et al.*, 1995). The development of electroactive materials for artificial muscles or actuators is sought after because of the benefits they offer.

Gelatin is a one type of electroactive polymers; it is protein a biopolymer derived from the partial hydrolysis of native collagens, the most abundant structural proteins found in the animal body: skin, tendons, cartilage, and bone. It is a good film and particle–forming material (Yang *et al.*, 1997). Due to its wealth of merits—its biological origin, non–immunogenicity, biodegradability, biocompatibility, and commercial availability at relatively low cost—gelatin has been widely used in the pharmaceutical and medical fields: sealants for vascular prostheses, carriers for drug delivery, wound dressings, and artificial muscles (Marois *et al.*, 1995). Normally Gelatin is produced by denaturing a naturally derived collagen in a solution through either acidic or alkaline process in which the triple-helix structure is separated into the random coil structure. During the gelling process, the random coil in a warm aqueous solution will change into the coil–helix structure when cooled (Ross-Murphy, 1992). However, gelatin exhibits poor mechanical properties, which limits its possible application as a biomaterial. In order to use this material in practical applications, the structure needs to be reinforced either through crosslinking or using some filler materials. However, the presence of residual crosslinking agents can lead to toxic side effects. The use of multiwall carbon–nanotube (MWNT) as a reinforcement in gelatin has been studied by Haider *et al.*(2007). Recently, the

insertion of a conductive polymer into a biopolymer forming a blend has been of keen interest. Conductive polymers can offer a variety of benefits to the host biopolymer: variable conductivity, better thermal stability, and mechanical properties (Puvanatvattana *et al.*, 2006). On the other hand, conducting polymers have been intensively studied for their one-dimensional conjugated structures and adjustable conductivity (Skotheim *et al.*, 1998). Conducting polymers can offer variety of benefits to our matrix: variable conductivity, better thermal stability, and mechanical properties. Among the conducting polymers, polypyrrole (Ppy) is one of the most investigated due to its high electrical conductivity, relatively good environmental stability, and low toxicity (Yang *et al.*, 2001; Athawale *et al.*, 2008; Waghuley *et al.*, 2008). Thus, the synthesis of nanoscale materials has attracted great interest during the past 10 years. Chemical oxidation polymerization is simple and cheap in producing large quantities of nanostructural polypyrrole (Ppy), because it overcomes the limitation of electrochemical polymerization. Duchet *et al.* (1998) used commercial polycarbonate nanoporous particle track-etched membranes as templates to prepare Ppynanotubules and nanofibrils (Duchet *et al.*, 1998).

In the present study, we are interested in blending of the nanowire-polypyrrole (nanowire Ppy) as a conductive polymer with a gelatin hydrogel containing an ionic surfactant (i.e., Dodecylbenzene sulfonic acid dispersed in an aqueous solvent). The mechanical properties, electromechanical properties, and electrical properties were investigated in terms of nanowire Ppy concentration, electric field strength, and temperature.

3.3 Materials and Methods

3.3.1 Materials

Gelatin (Type B, bovine skin), Pyrrole monomer (Sigma), Calcium hydride (CaH_2, Fluka) were used as received. Anhydrous iron(III) chloride ($FeCl_3$, Riedel-de Hean) was used as an oxidant without further purification. Dodecylbenzene sulfonic acid (DBSA, Sigma) was used as received and as a dopant.

3.3.2 Synthesis of Nanowire-polypyrrole

In this work, we followed the chemical synthesis procedure of He *et al.* (2003) for the nanowire Ppy. The pyrrole monomer was dried by mixing with CaH_2 at a ratio of 100 g of CaH_2 per litre of pyrrole and the reaction was allowed to proceed for 24 h. 0.0175 mol of dodecylbenzene sulfonic acid and 0.0175 mol of dried pyrrole monomer were dissolved into separate beakers of 250 ml of distilled water. Then, the solutions were mixed together by vigorously stirring to obtain an emulsion. A solution of $FeCl_3$ (0.065 mol, 0.01625 M) in deionized water was added to the emulsion at 0 °C for a duration of 40 h. It was terminated by pouring a large excessive methanol into the solution. Then, the resulting polypyrrole precipitate was vacuum-filtered and washed with methanol, acetone, and distilled water several times until pH was equal to 6.0. Finally, it was dried in a vacuum oven for 40 h at 30 °C.Other Ppys were synthesized with the same procedure but with 0.000175, 0.00175, 0.175, 0.875, and 1.75 mols of DBSA.

3.3.3 Preparation of Nanowire-polypyrrole/Gelatin Hydrogel

The various concentrations of nanowire Ppy: 0.01, 0.1, 0.5, and 1%v/v were dispersed by a transonicator (Elma, D 7284) in an aqueous medium filled with 4×10^{-3} M of DBSA. Then the gelatin hydrogel was prepared via the dissolution in the 10 %v/v in distilled water (pH = 6.40) at 40 °C overnight by magnetic stirring until pH was equal to 6.31. The two solutions were mixed and poured onto a petri dish for the hydrogel casting at a room temperature. The thickness of hydrogel samples was about 1.4 mm. Fig. 3.1 shows a schematic for the possible interaction of the gelatin and dodecylbenzene sulfonic acid (DBSA).

3.3.4 Characterization and Testing of Hydrogel Composites

Each polypyrrole sample was identified for functional groups by a Fourier transform infrared spectroscopy (Thermo Nicolet, Nexus 670) operated in the absorption mode with 32 scans and a resolution of ±4 cm^{-1}, covering a wavenumber range of 3500 cm^{-1} to 500 cm^{-1} using a deuteratedtriglycine sulfate detector. Optical grade potassium bromide (KBr, Carlo Erba Reagent) was used as the background material.

Electrical conductivity was measured by a meter which consists of two probes that make contact with the surface of the film sample. The probes were connected to a source meter (Keithley, Model 6517A) for a constant voltage source and for read ability of the current. The applied voltage and the resultant current in the linear Ohmic regime were used to determine electrical conductivity of the polymer using Equation (3.1) as follows:

$$\sigma = \frac{1}{\rho} = \frac{1}{R_s t} = \frac{1}{KVT} \tag{3.1}$$

where σ is the specific conductivity (S/cm), ρ is the specific resistivity (Ω cm). R_s is the sheet resistivity (Ω), I is the measured current (A), K is the geometric correction factor, V is the applied voltage (V), and t is the pellet thickness (cm).

Scanning electron micrographs were taken with a scanning electron microscope (JEOL, model JSM-5200) to determine the morphology of the polypyrrole in a powder form at various DBSA concentrations. The scanning electron micrographs of polypyrrole were obtained by using an acceleration voltage of 15 kV with magnifications of 15 000 and 100 000 times.

Atomic force microscopy (AFM, CSPM 4000) images were taken with a scanning electron microscope to determine the topology of the hydrogels at various concentrations of nanowire Ppy by using a scan rate 0.5 Hz and a scan size 10 μm x 10 μm.

A melt rheometer (Rheometric Scientific, ARES) was used to measure the rheological properties. It was fitted with a custom-built copper parallel plate fixture (diameter of 30 mm). A DC voltage was applied with a DC power supply (Instek, GFG8216A), which can deliver electric field strength to 800 V/mm. A digital multimeter was used to monitor the voltage input. In these experiments, the oscillatory shear strain was applied and the dynamic moduli (G' and G'') were measured as functions of frequency and electric field strength. Strain sweep tests were first carried out to determine suitable strains to measure the G' and G'' in the linear viscoelastic regime. The appropriate strain was determined to be 0.15 % for both the pure gelatin hydrogels and for the nanowire Ppy/gelatin hydrogels. Then

frequency sweep tests were carried out to measure G' and G'' of each sample as functions of frequency. The deformation frequency was varied from 0.1 to 100 rad/s. Before each measurement, pure gelatin hydrogels and nanowire Ppy/gelatin hydrogels were presheared at a low frequency (0.039811 rad/s), and then the electric field was applied for 15 min to ensure the formation of equilibrium polarization before taking the G' and G'' measurements. Experiments were carried out at a temperature of 30 °C and repeated at least two to three times. The effect of temperature was studied at various temperatures between 30 and 80 °C for the pure gelatin hydrogels and the nanowire Ppy/gelatin hydrogels. The temporal response experiments were carried out at 800 V/mm for the pure gelatin hydrogels and the nanowire Ppy/gelatin hydrogels. Deflections of the pure gelatin hydrogel and the nanowire Ppy/gelatin hydergels were carried out under various applied electric strengths. For each hydrogel, one end of the sample was fixed with a grip vertically in a transparent chamber containing two parallel electrodes. The input DC field was provided by a DC power supply (Gold Sun 3000, GPS 3003D) and a high voltage power supply (Gamma High Voltage, UC5-30P), which delivered various electric field strengths, from 25 to 600 V/mm. A digital video recorder (Sony, Handicam HR1) was used to record the displacement of the films. The tip displacement was measured and calculated from a Scion Image (Beta 4.0.3) program.

From the static force balance, the deflecting force or the dielectrophoresis force (F_d) on the samples is equal to the sum of the resisting elastic force (F_e) and the weight along the bending direction Equation (3.2), where the film deflection distance at equilibrium is d.

$$F_d = F_e + mg \sin \theta \tag{3.2}$$

where m is the sample's mass (kg), g is the gravity constant (9.8 m/s^2), θis the deflection angle, and F_e is the resisting elastic force (N). In our experiment, the film deflections were small. The linear deflection theory of one free-end film is, therefore, used where the elastic force can be calculated by the following equation (3.3) (Sato *et al.*, 1996; Timoshenko *et al.*, 1970):

$$F_e = \frac{dEI}{l^3} \tag{3.3}$$

where E is the elastic modulus which is equal to 2G′(1+ν) in which G′(1 rad/s, E) is the shear modulus and ν is the Poisson's ratio, which is equal to 1/2 for an incompressible material, I is the moment of inertia, equal to $t^3w/12$, where t is the sample thickness, w is the sample width, d is the deflection distance, and l is the sample length.

3.4 Result and Discussion

3.4.1 Characterization of Nanowire Polypyrrole

A FT-IR spectrum of the Ppy was taken to identify the characteristic absorption peaks as shown in table 1, the characteristic peaks of the synthesized Ppy are at 1547, 1450, 1302, 1178, 1038, and 633 cm^{-1}. The pyrrole ring vibration occurs at 1547 and 1450 cm^{-1}, the =C-H in plane vibration at 1302 and 1038 cm^{-1} (He *et al.*, 2003), the C-N stretching vibration at 1178 cm^{-1} (Prissanaroon *et al.*, 2000). When Ppy is doped with DBSA, the peak at 633 cm^{-1} increases. This peak represents the S=O and S-O stretching vibrations of sulfonate anions which compensate for the positive charges in the Ppy chains (Diaz *et al.*, 1983).

The effect of the doping level on the morphology of the conductive polymer was investigated by Scanning electron microscopy (SEM). Figures 3.2(a)–(c) show SEM micrographs of synthesized Ppy of various DBSA concentrations: 0.00175 to 1.75 mol (N_{DBSA}:$N_{monomer}$ equal to 0.01:1, 0.1:1, 0.5:1, 1:1, 5:1, and 10:1). It is interesting to observe that upon increasing the dopant level, the morphology of the conductive polymer changes from having typical three dimensional random coil nanogranular structures to nanowire fibrillar structures and then return to a nanogranular structure again (Fig. 3.2(a)–(c)). The micrographs suggest that as the dopant concentration increases more polarons and bipolarons are generated along the polymer chains and they induce a glanule-to-nanowire transition. It can be seen that the concentration of DBSA strongly affects the

morphology of the Ppy obtained. When the concentration of DBSA in the reaction solution is higher than 0.175 mol, the resulting morphology of polypyrrole is the granular, similar to those of the Ppy synthesized with other dopants (Diaz *et al.*, 1983; Street *et al.*, 1985; Shen *et al.*, 1998). As previously mentioned, the nanowire Ppy was obtained when the reacting solution was at a proper reactant concentration, and the nanogranular Ppy was obtained with a higher reactant concentration (Kwon *et al.*, 2008). The resulting Ppy averaged particle sizes of various DBSA concentrations (N_{DBSA}:$N_{monomer}$ equal to 0.01:1, 0.1:1, 0.5:1, 1:1, 5:1, and 10:1) are tabulated in table 3.2. Figures 3.3(a)–(c) show the SEM micrographs of the cross-sections of the nanowire Ppy/Gelatin hydrogels at various nanowire Ppy concentrations. The nanowire Ppy shows a moderate dispersion in the gelatin solution at low nanowire Ppy concentrations with the aid of the surfactant; the dispersion becomes relatively poor at high nanowire Ppy concentrations. Partially homogeneous nanowire Ppy/gelatin hydrogel is obtained due to the poor nanowire Ppy dispersion as a result of the van der Waals forces between Ppy nanowires.

The specific electrical conductivity of Ppy and the nanowire Ppy were measured with a custom-built two point probe (Keithley, Model 6517A). The specific electrical conductivity with corresponding standard deviations of Ppy, at N_{DBSA}:$N_{monomer}$ equal to 0.01:1, 0.1:1, 0.5:1, 1:1, 5:1, and 10:1, are shown in table 3.2. The electrical conductivity of Ppy is thus closely related to their morphology. The conductivity (σ) is expressed as $\sigma = ne\mu$ where "n" is the density of the charge carrier, "e" represents the electron charge, and μ is the mobility of the charge carrier. Thus, the electrical conductivity of Ppy is proportional to the density (the doping level in the case of conducting polymers) and the mobility of the charge carriers. The conductivity of the nanogranular Ppy (10:1) is 15.95 S/cm, lower than the nanowire Ppy (1:1) which is 23.86 S/cm. The Ppy with the nanowire morphology presumably has a higher mobility for the charge carriers than that of the granular Ppy and this factor dominates the charge carrier density factor (Martin, 1994).

The topology and the orientation of the nanowire Ppy /gelatin hydrogels were also investigated by AFM. The AFM micrographs of the nanowire Ppy/gelatin and the pure gelatin hydrogels are demonstrated in Fig. 3.4(a)–(c).Fig. 3.4(a) shows the topology and the orientation of the 0.1 %v/v nanowire Ppy/gelatin

hydrogel; it consists of nanorods which are aligned in one direction with a uniform distribution by a mechanical force; the schematic diagram is illustrated in Fig. 3.4(a′). The 1% nanowire Ppy/gelatin hydrogel possesses a cottage–like topology. Its topology presumably consists of nanowires piling up randomly with each other as shown in the schematic diagrams of Fig. 3.4(b) and Fig. 3.4(b′) due to the agglomeration. The last illustration is of the pure gelatin hydrogel as shown in Fig. 3.4(c).Fig. 3.4(a) of the 0.1 %v/v nanowire Ppy/gelatin hydrogel shows that the nanowire Ppy are dispersed quite uniformly within the gelatin hydrogel.

3.4.2 Electromechanical Properties

3.4.2.1 Time Dependence of Electrorheological Response

We investigated the temporal characteristics of the pure gelatin and the nanowire Ppy/gelatin hydrogels (0.1 %v/v and 1 %v/v) at an electric field strength of 800 V/mm from the time sweep tests, in which the electric field was turned on and off alternately. The temporal characteristic of each sample was recorded in the linear viscoelastic regime at a strain of 0.15 %, and a frequency of 100 rad/s. Fig. 3.5 shows the comparison in the storage modulus, G′ of the pure gelatin and of the nanowire PPp/gelatin hydrogels, during the time sweep tests. At the electric field strength of 800 V/mm, G′ immediately increases and rapidly reaches a steady-state value. For the pure gelatin hydrogel, as the electric field is turned off, G′ decreases instantaneously to its original state. For the nanowire Ppy/gelatin hydrogel (0.1 %v/v, and 1 %v/v), G′ decreases but does not recover its original value. This behavior indicates that there are some irreversible agglomerations of the nanowire Ppy or some dipole moment residues, possibly due to some hydrogen bonding between adjacent nanowire Ppy. However, the 1% v/v naonowire Ppy/gelatin hydrogel shows a quick response under an electric field since the agglomeration of nanowire Ppy in hydrogels constitutes large induced dipole moment domains.

3.4.2.2 Effect of Electric Field Strength and Concentration

The effect of electric field strength on the electromechanical properties of the nanowire Ppy/gelatin hydrogels of 0, 0.01, 0.1, 0.5, and 1 vol% were investigated in a range of 0 to 800 V/mm. Fig. 3.6 shows the storage modulus response ($\Delta G'$) of the hydrogels vs. electric field strength at a frequency of 100 rad/s, a strain of 0.15 %, and at a temperature of 30 °C. The increases in $\Delta G'$ with electric field strength are nonlinear within the range of 0.1 to 800 V/mm. The storage modulus response values of these samples at an electric field strength of 800 V/mm are 250 000, 503 000, 1 005 000, 212 990, and 202 779 Pa for the pure gelatin, the nanowire Ppy 0.01 vol%/gelatin, the nanowire Ppy 0.1 vol%/gelatin, the nanowire Ppy 0.5vol%/gelatin, and the nanowire Ppy 1 vol%/gelatin hydrogels, respectively. (The storage modulus sensitivity values of these samples at an electric field strength of 800 V/mm are tabulated in Table 1) The mixing of the nanowire Ppy into gelatin leads to the increases in G' with and without an electric field. The increase of G'_o can be attributed to the effect of particles acting as fillers. For the small amount of nanowire Ppy added, the fillers induce only an additional free volume, but the distances between particles are large enough to create a significant particle interaction through the electric field-induced dipole moments (Shiga, 1997). Therefore, the storage modulus sensitivity becomes high only at suitable nanowire Ppy concentrations. The maximum $\Delta G'$ and $\Delta G'/G'_o$ occurs with the nanowire Ppy 0.1 vol%/gelatin hydrogel. However, the storage modulus response and sensitivity decrease with the nanowire Ppy concentration greater than 0.1 vol%. For the hydrogel system with the highest particle concentration of 1 vol%, the storage modulus response under the effect of the electric field diminishes since the hydrogel presumably consists of the phase separation between the gelatin hydrogel and the nanowire Ppy agglomeration.

Liu *et al.* (2001) reported a similar effect for a silica/silicone system. The enhancement of shear modulus was negligible below 8.0 vol%, but increased dramatically above this threshold concentration. At a volume amount above 55 vol%, the shear modulus decreased since the interparticle force decreased with the steric hindrance effect (Liu *et al.*, 2001). Kunanuruksapong *et al.* (2007) found that the storage moduli of a polymer blend between poly(*p*-phenylene) and an

acrylic elastomer increased with increasing poly(*p*-phenylene) concentration. However at the higher particle concentration of 30 vol%, the storage modulus response ($\Delta G'_{2kV/mm}$) decreased (Kunanuruksapong *et al.*, 2007).

3.4.2.3 Effect of Operating Temperature

The mechanical properties under an electric field of the pure gelatin and the nanowire Ppy/gelatin hydrogels were investigated at operating temperatures between 30 and 80 °C. G' and $\Delta G'$ (100 rad/s) are plotted with temperature as shown in Fig. 3.7. One sample was used for each of the G'_0 and G' measurements. An electric field was first applied on another sample for a period of 10 min before G' was measured successively at each temperature. Experiments were carried out using two representative hydrogels—Pure gelatin and nanowire Ppy 0.1 vol%/gelatin hydrogel as shown in Fig. 3.7. Figure 3.7 shows the storage modulus of the pure gelatin hydrogel initially decreases in the temperature range of 30–40 °C because of the denaturation of the triple helix coil to the random coil (Bigi *et al.*, 2004). In the temperature range of 40–60 °C, the storage modulus increases, consistent with the classical network theory (Sato *et al.*, 1996). A higher temperature induces more entropy of the gel, leading to the increase in the retractive force and the storage modulus. However the storage modulus decreases with increasing temperature between 60–80 °C, the temperature range close to the low-temperature glasss transition of 120 °C in which the devitrification of α-amino acid block occurs (Fraga *et al.*, 1985). In the case of 0.1 vol% nanowire-Ppy/gelatin hydrogel, the temperature increment under electric field retards the denaturation temperature (30–40 °C) and the low-temperature glass transition (60–80 °C) because of the polarization of Ppy. In addition, the storage modulus increment drastically increases with temperature consistent with the classical network theory (40–60 °C). From the results shown, the electromechanical responses of nanowire-Ppy/gelatin hydrogel are mainly improved in terms of storage modulus response ($\Delta G'$) via the Ppy polarization. With the presence of nanowire Ppy, $G'_{800w/mm}$ and $\Delta G'$ at any temperature are higher than those of the pure gelatin hydrogel since the nanowire Ppy acts as a filler and creates the wire-to-wire dipole interaction under the electric field.

3.4.3 Deflection of Nanowire Ppy/Gelatin Hydrogels

The deflection of the pure gelatin and nanowire Ppy/gelatin hydrogels were studied by vertically suspending the films in a silicon oil bath; and a DC electric field was applied horizontally between two parallel flat copper electrodes, as shown in Fig. 3.8. The amount of deflection at a specified electric field strength is defined by the geometrical parameters—d, l, and θ—which are illustrated in Fig. 3.8. The tip displacement of the film was recorded by a digital video recorder (Sony, Handicam HR1). Figures 3.9(a)–(c) show the bendings of the pure gelatin and the nanowire Ppy/gelatin hydrogels immersed in the silicone oil under an electric field strength of 600 V/mm. Upon applying an electric field, the free lower end of the film deflects towards the anode side by an amount dependent on the field strength that result from the effect of the non-symmetric charges. The pure gelatin hydrogel indicates an attractive interaction between the anode and the polarlized carboxyl group, in which the gelatin structure possesses negative charges. The deflection distances of the pure gelatin and the nanowire Ppy/gelatin hydrogels under the electric field are shown in Fig. 3.10(a)–(b). The pure gelatin hydrogel shows greater deflection values than those of the nanowire Ppy/gelatin hydrogels. The hydrogels start to deflect at lower critical electric field strengths 25 V/mm, 300 V/mm, and 400 V/mm for the pure gelatin hydrogel, the nanowire Ppy 0.1 vol%/gelatin, and the nanowire Ppy 1vol%/gelatin hydrogel, respectively. Moreover, the nanowire Ppy/gelatin hydrogels has a lesser deflection response under the applied electric field than the pure gelatin hydrogel due to its initial higher rigidity, or its higher G'_o value.

Figures 3.10(a)–(b) show the deflection distances and the dielectrophoresis forces of the pure gelatin and the nanowire Ppy/gelatin hydrogels under an electric field. The deflection distances and dielectrophoresis forces of the pure gelatin and nanowire Ppy/gelatin hydrogels appear to increase stepwise with increasing electric field strength. The dielectrophoresis forces at E = 600 V/mm force of the pure gelatin hydrogel, nanowire Ppy 0.1 vol%/gelatin, and nanowire Ppy 1.0 vol%/gelatin hydrogel are 7.05, 6.60, and 1.60 mN, respectively. Surprisingly, the resultant dielectrophoresis forces of the nanowire Ppy/gelatin hydrogels under the applied electric field are smaller than those of the pure gelatin hydrogel. It appears that the induced dipole moments generated by nanowire Ppy counteract with those of

the pure gelatin. Under an applied electric field, pure gelatin hydrogel can polarize and generate non-symmetric negative charges. On the other hand, the nanowire Ppy has strong positive charges attached on the main chains. Apparently, the presence of positive charges diminishes the non-symmetric negative charges generated within the gelatin matrix. Therefore, the bending and the dielectrophoresis forces of the nanowire Ppy/gelatin hydrogels under electric field are less.

In previous work, Thongsak *et al.* (2010) reported the dielectrophoresis force of styrene-isoprene-styrene triblock copolymer (SIS D1114P), the maximum deflection distance, and the dielectrophoresis force at E = 600 V/mm was 2.86 mm and 36.4 μN, respectively (Thongsak *et al.*, 2010). Dai *et al.* (2009) studied the bending force under applied electric field of ionic network membrane based on the blends of water soluble poly vinyl alcohol (PVA) and highly ionic conductive poly 2-acrylamido-2-methyl-1- propanesulfonic acid (PAMPS). The bending force of the PVA/PAMPS blend was equal to 4.9 mN at E = 40 V/mm (Dai *et al.*, 2009). Kunanuruksapong *et al.* (2011) studied the electromechanical response of an acrylic elastromer (AR70). The maximum deflection distance and dielectrophoresis force at the electrical strength of 225 V/mm was 12.41 mm and 0.367 mN, respectively (Kunanuruksapong *et al.*, 2011).For the pure gelatin and nanowire PPy/gelatin hydrogels studied in this work, the maximum deflection distance and dielectrophoretic force were obtained for the pure gelatin hydrogel at E = 600 V/mm. They were 14.84 mm and 7.055 mN, respectively.

3.5 Conclusions

In this study, the electromechanical properties, the storage modulus response under oscillatory shear mode and the cantilever bending, of pure gelatin and nanowire Ppy/gelatin hydrogels were investigated as functions of electric field strength and operating temperature. In the pure gelatin hydrogel and nanowire Ppy/gelatin hydrogels 0.01, 0.1, 0.5, and 1 vol%., the storage modulus (G'), the storage moduli response ($\Delta G'$) and the storage modulus sensitivity ($\Delta G'/G_0$) increase monotonically with increasing electric field strength up to 800 V/mm. The maximum storage modulus sensitivity was 104% for the nanowire Ppy 0.1 vol% / gelatin

hydrogel at an electric field strength of 800 V/mm. The mechanism for the storage modulus response is the interaction between electrically polarized nanowire Ppy which induces an electrostatic interaction and the effect of particles acting as fillers. Under the presence of nanowire Ppy, G' and $\Delta G'$ at any temperature investigated are higher than those of the pure gelatin hydrogel since the nanowire Ppy acts as a filler and creates the wire-to-wire dipole interaction under the electric field. For the deflection measurement, the deflection distances and the dielectrophoresis forces of the pure gelatin and nanowire Ppy/gelatin hydrogels increase monotonically with increasing electric field strength. In the case of the nanowire Ppy 1 vol%/gelatin hydrogel it possesses the lowest deflection response relative to others due to its initially higher rigidity or its higher G'_o value. However, the nanowire Ppy 0.1 vol%/gelatin hydrogel is shown overall here to be more electroactive than the pure gelatin hydrogel.

3.6 Acknowledgements

The authors would like to acknowledge the TRF-RGJ and TRF-BRG, The Center of Petroleum Petrochemical and Advance Materials, The Conductive & Electroactive Polymer Research Unit of Chulalongkorn University, and The Royal Thai Government (Budget of Fiscal Year 2552).

3.7 References

Athawale, A.A., Katre, P.P., Bhagwat, S.V., and Dhamane, A.H. (2008) Synthesis of polypyrrolenanofibers by ultrasonic waves. Journal of Applied Polymer Science, 108, 2872-2875.

Bar-Cohen, Y. (2004) Electroactive Polymer (EAP) as Artificial Muscles: Reality, Potential, and Challenges, 2nd ed. Bellingham, Washington: SPIE Press.

Bigi, A., Panzavolta, S., and Rubini, K. Relationship between triple-helix content and mechanical properties of gelatin films. Biomaterials, 25, 5675-5680.

Calvert, P. and Liu, Z. (1998) Freeform fabrication of hydrogels. Acta Materialia, 46, 2565-2571.

Dai, C.A., Kao, A., Chang, C., Tsai, W., Chen, W., Liu, W., Shih, W., and Ma, C.C. (2009) Polymer actuator based on PVA/PAMPS ionic membrane: Optimization of ionic transport properties. Sensors and Actuators A: Physical, 155, 152-162.

Diaz, F. and Hall, B. (1983) Mechanical properties of electrochemically prepared polypyrrole films. IBM Journal of Research and Development, 27, 342-347.

Duchet, J., Legras, R., and Demousteir-Champagne, S. (1998) Chemical synthesis odpolypyrrole: structure-properties relationship. Synthetic Metals, 98, 113-122.

Fraga, A.N. and Williams, R.J.J. (1985) Thermal properties of gelatin films. Polymer, 26, 113-118.

Haider, S., Park, S.Y., Saeed, K., and Farmer, B.L. (2007) Swelling and electroresponsive characteristics of gelatin immobilized onto multi-walled carbon nanotubes. Sensors and Actuators B: Chemical, 124, 517-528.

He, C., Yang, C., and Li, Y. (2003) Chemical synthesis of coral-like nanowires and nanowire networks of conducting polypyrrole. Synthetic Metals, 139, 539-545.

Kim, J. and Seo, Y.B. (2002) Electro-active paper actuators. Smart Materials and Structures, 11, 355-360.

Koyama, K., Minagawa, K., Watanabe, T., Kumakura, Y., and Takimoto, J. (1995) Electro-magneto-rheological effects in parallel-field and crossed-field systems. Journal of Non-Newtonian Fluid Mechanics, 58, 195-206.

Kunanuruksapong, R. and Sirivat, A. (2007) Poly(p-phenylene) and acrylic elastomer blends for electroactive application. Material Science and Engineering: A, 454-455, 453-460.

Kunanuruksapong, R. and Sirivat, A. (2011) Effect of dielectric constant and electric fiels strength on dielectrophoresis force of acrylic elastomers and styrene copolymers. Current Applied Physics, 11, 393-401.

Kwon, W.J., Suh, D.K., Chin, B.D., and Yu, J.W. (2008) Preparation of polypyrrole nanoparticles in mixed surfactants system. Journal of Applied Polymer Science, 110: 1324-1329.

Liu, B. and Shaw, T.M. (2001) Electrorheology of filled silicone elastromers. Journal of Rheology, 45, 641-657.

MacDiarmid, A.G., Chiang, J.C., Halpern, M., Huang, W.S., Mu, S.L., Somasiri, N.L., Wu, W.Q., and Yaniger, S.I. (1985) Polyaniline: Interconversion of metallic and insulating forms. Molecular Crystals and Liquid Crystals, 121, 173-180.

Marois, Y., Chakfe, N., Deng, X., Marois, M., How, T., King, M.W., and Guidoin, R. (1995) Carbodiimide cross-linked gelatin: a new coating for porous polyester arterial prostheses. Biomaterials, 16, 1131-9.

Martin, C.R. (1994) Nanomaterials: a membrane-based synthetic approach. Science, 266, 1961-1966.

Perline, R.E., Kornbluh, R.D., and Joseph, J.P. (1998) Electrostriction of polymer dielectrics with compliant electrodes as a means of actuation. Sensors Actuators A: Physical, 64, 77-85.

Prissanaroon, W., Ruangchuay, L., Sirivat, A., and Schwank, J. (2000) Electrocal conductivity response of dodecylbenzene sulfonic acid-doped polypyrrole film to SO2-N2 mixtures. Synthetic Metals, 114, 65-72.

Puvanatvattana, T., Chotpattananont, D., Hiamtup, P., Niamlang, S., Sirivat, A., and Jamieson, A.M. (2006) Electric field induced stress moduli in

polythiophene/polyisopreneelastromer blends. Reactive and Functional Polymers, 66, 1575-1588.

Ross-Murphy, S.B. (1992) Structure and rheology of gelatin gels: recent progress. Polymer, 33, 2622-2627.

Sato, T., Watanabe, H., and Osaki, K. (1996) Rheological and dielectric behavior of a stylene-isoprene-styrene triblock copolymer inn-tetradecane. 1. Rubbery-plastic-viscous transition. Macromolecules, 29, 6231-6239.

Shahinpoor, M., Bar-Cohen, Y., Simson, J.O., and Smith, J. (1998) Ionic polymer-metal composites (IPMCs) as biomimetic sensors, actuators and artificial muscles – a review. Smart Materials and Structures, 7, 15-30.

Shen, Y. and Wan, M. (1998) In situ doping polymerization of pyrrole with sulfonic acid as a dopant. Synthetic Metals, 96, 127-132.

Shiga, T. (1997) Deformation and Viscoelastic Behavior of Polymer Gels in Electric Fields, Advances in Polymer Science. Berlin: Springer-Verlag.

Skotheim, T.A., Elsenbaumer, R.L., Reynolds, J.R. (1998) Handbook of Conducting Polymers, 2nd ed., New York: Marcel Dekker.

Street, G.B., Lindsey, S.E., Nazzal, A.I., and Wynne, K.J. (1985) The Structure and mechanical properties of polypyrrole. Molecular Crystals and Liquid Crystals, 118, 137-148.

Thongsak, K., Kunanuruksapong, R., Sirivat, A., and Lerdwijitjarud, W. (2011) Electroactivepolydiphenylamine/poly(styrene-block-isoprene-block-styrene) (SIS) blends: Effects of particle concentration and electric field. Materials Science and Engineering: C, 31, 206-214.

Timoshenko, S.P., and Goodier, J.N. (1970) Theory of Elasticity, 3rd ed. Auckland: McGraw-Hill.

Waghuley, S.A., Yenorkar, S.M., Yawale, S.S., and Yawale, S.P. (2008) Application of chemically synthesized conducting polymer-polypyrrole as a carbon dioxide gas sensor. Sensors and Actuators B: Chemical, 128, 366-373.

Yang, X.J., Zheng, P.J., Cui, Z.D., Zhao, N.Q., Wang, Y.F., and Yao, K.D. (1997) Swelling behavior and elastic properties of gelatin gels. Polymer International, 44, 448-452.

Yang, Y. and Wan, M. (2001) Microtubules of polypyrrole synthesized by an electrochemical template-free method. Journal of Materials Chemistry, 11, 2022-2027.

Zhang, Q.M., Bharti, V., and Zhao, X. (1998) Giant electrostriction and relaxor ferroelectric behavior in electron-irradiated poly(vinylidene fluoride-trifluoroethylene) copolymer. Science, 280, 2101-2104.

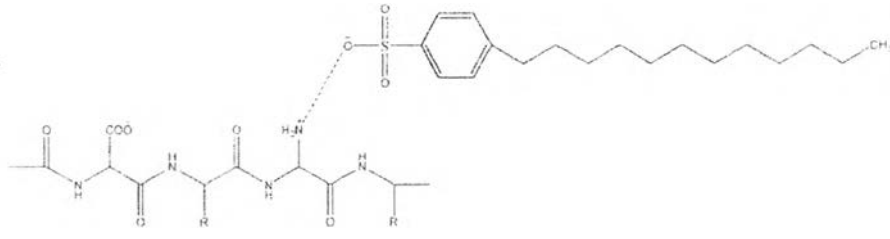

Figure 3.1 Scheme of the possible interaction of the gelatin and dodecylbenzene sulfonic acid (DBSA).

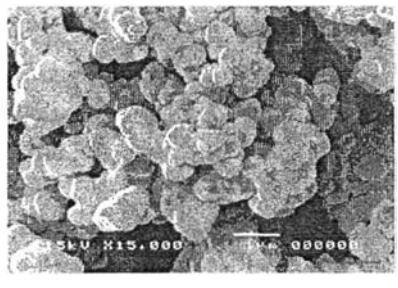

a) 0.00175 mol DBSA
(N_{DBSA}:$N_{monomer}$ = 0.01:1)

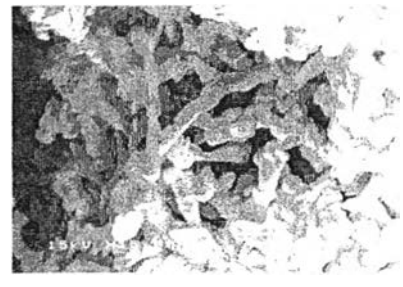

b) 0.175 mol DBSA
(N_{DBSA}:$N_{monomer}$ = 1:1)

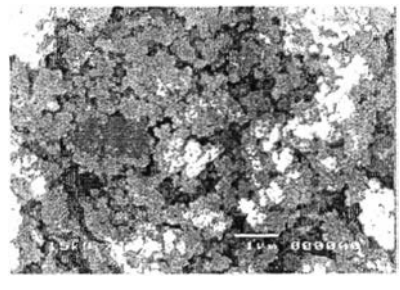

c) 1.75 mol DBSA
(N_{DBSA}:$N_{monomer}$ = 10:1)

Figure 3.2 SEM micrographs of DBSA-doped synthesized polypyrroles at various DBSA concentrations with a magnification of: (a) 0.0175 mol (N_{DBSA}:$N_{monomer}$ = 0.01:1); (b) 0.175 mol (N_{DBSA}:$N_{monomer}$ = 1:1); (c) 1.750 mol (N_{DBSA}:$N_{monomer}$ = 10:1).

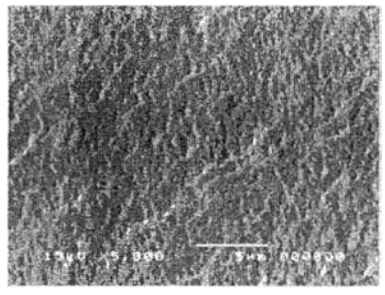

a) Cross-section of pure gelatin

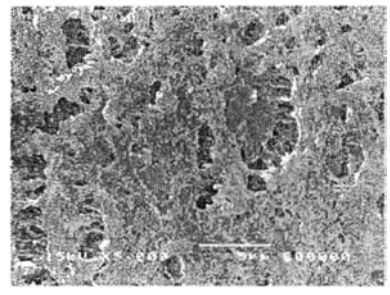

b) Cross-section of nanowire PPy0.1 %v/v / gelatin

c) Cross-section nanowire PPy1 %v/v / gelatin

Figure 3.3 SEM micrographs of cross-sections of the pure gelatin and the nanowire Ppy/Gelatin hydrogels; (a) cross-section of the pure gelatin; (b) cross-section of the 0.1 vol% nanowire Ppy/gelatin; and (c) cross-section of the 1 vol% nanowire Ppy/ gelatin.

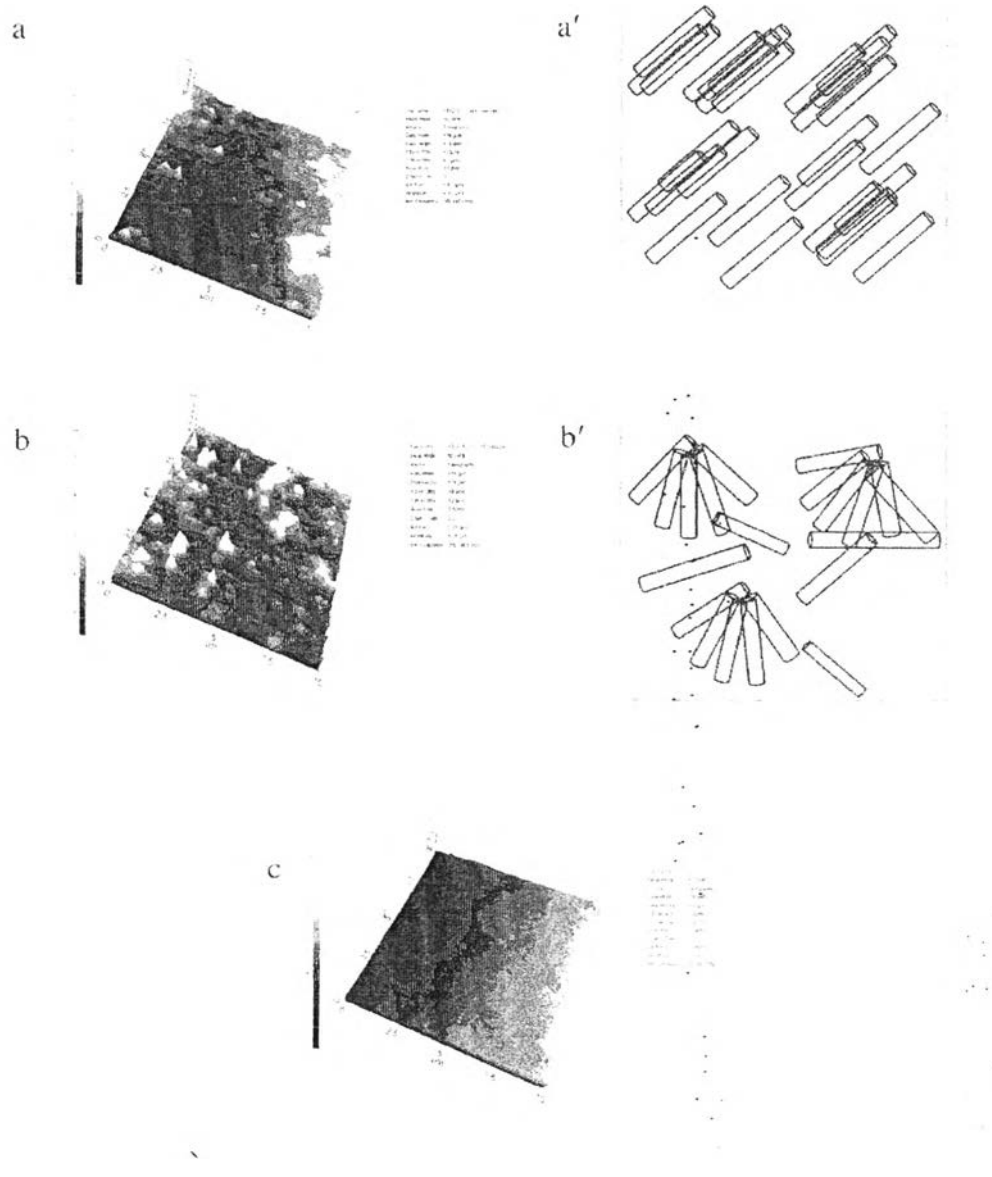

Figure 3.4 AFM micrographs of: (a) Nanowire Ppy 0.1 vol% /gelatin hydrogel; (a') Schematic diagram of nanowire Ppy 0.1 vol% orientation; (b) Nanowire Ppy 1 vol% /gelatin hydrogel; (b') Schematic diagram of nanowire Ppy 1 vol% orientation; and (c) Pure gelatin hydrogel.

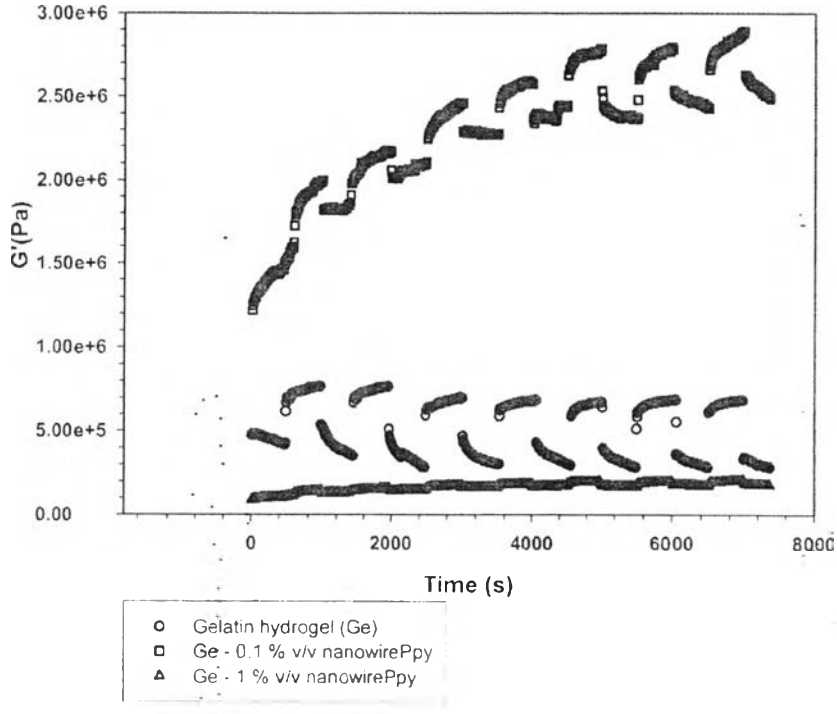

Figure 3.5 Temporal responses of the storage modulus (G') of the pure gelatin hydrogel and the nanowire Ppy/gelatin hydrogels (sample diameter 30 mm, gel thickness 1.405 mm, 0.15 % strain, frequency of 100 rad/s, electric field strength 800 V/mm, and at 30 °C):(○) pure gelatin hydrogel; (□) 0.1 %v/v nanowire Ppy; (Δ) 1 %v/v nanowire Ppy.

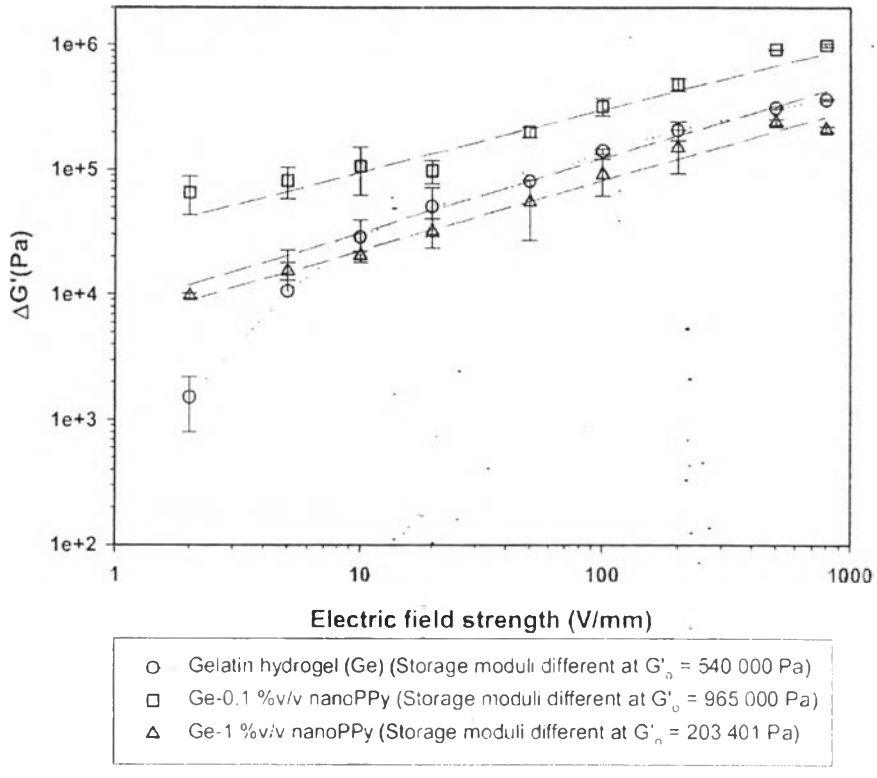

Figure 3.6 Effect of concentration of particles on the storage modulus response ($\Delta G'$) at various electric field strengths (sample diameter 30 mm, gel thickness 1.405 mm, 0.15 % strain, frequency of 100 rad/s, and at 30 °C): (○) Pure gelatin hydrogel; (□) 0.1 %v/v nanowire Ppy; and (Δ) 1%v/v nanowire Ppy.

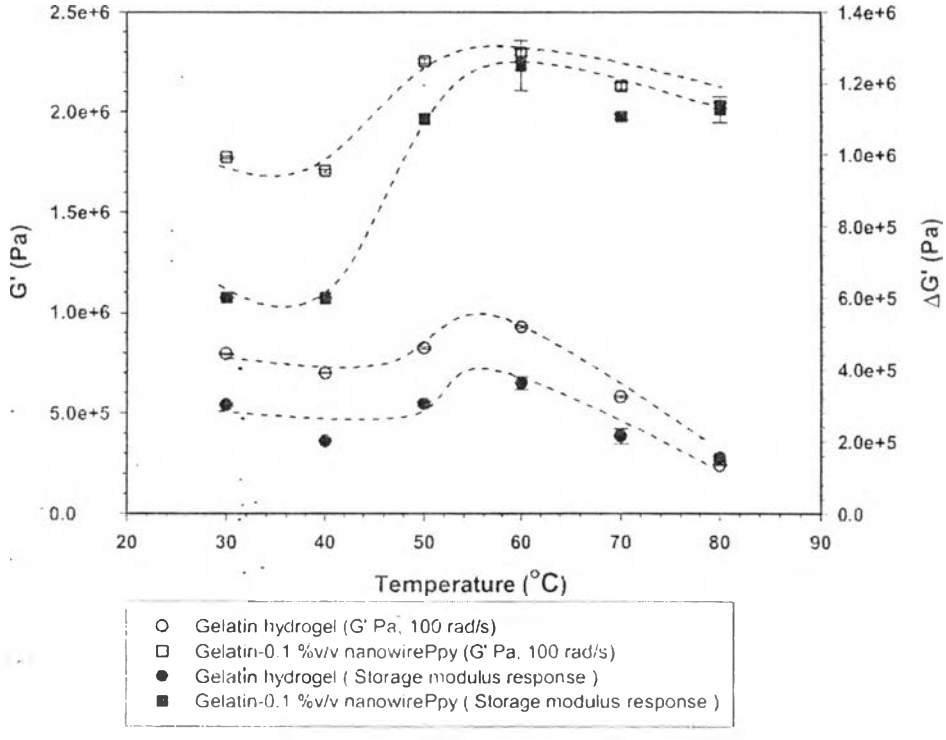

Figure 3.7 Effect of concentration of particles on the storage modulus (G') and the storage modulus response ($\Delta G'$) at various temperatures (sample diameter 30 mm, gel thickness 1.405 mm, 0.15 % strain, electric field strength 800 V/mm, frequency of 100 rad/s).

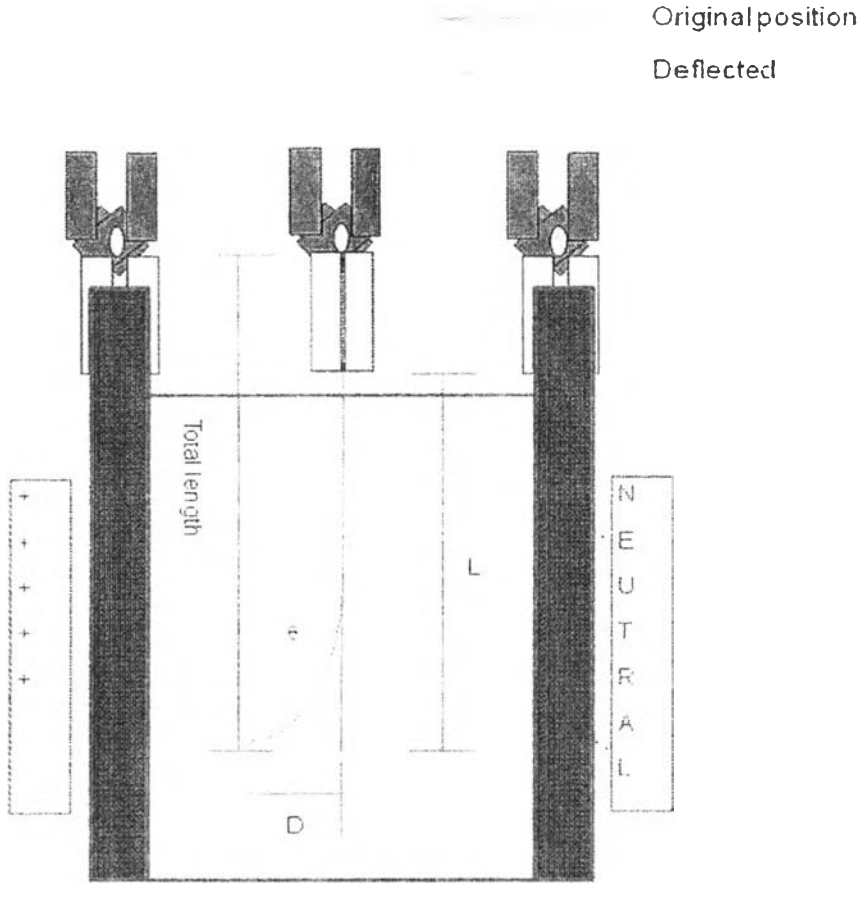

Figure 3.8 Schematic of the apparatus used to observe the dielectrophoretics on the hydrogel samples.

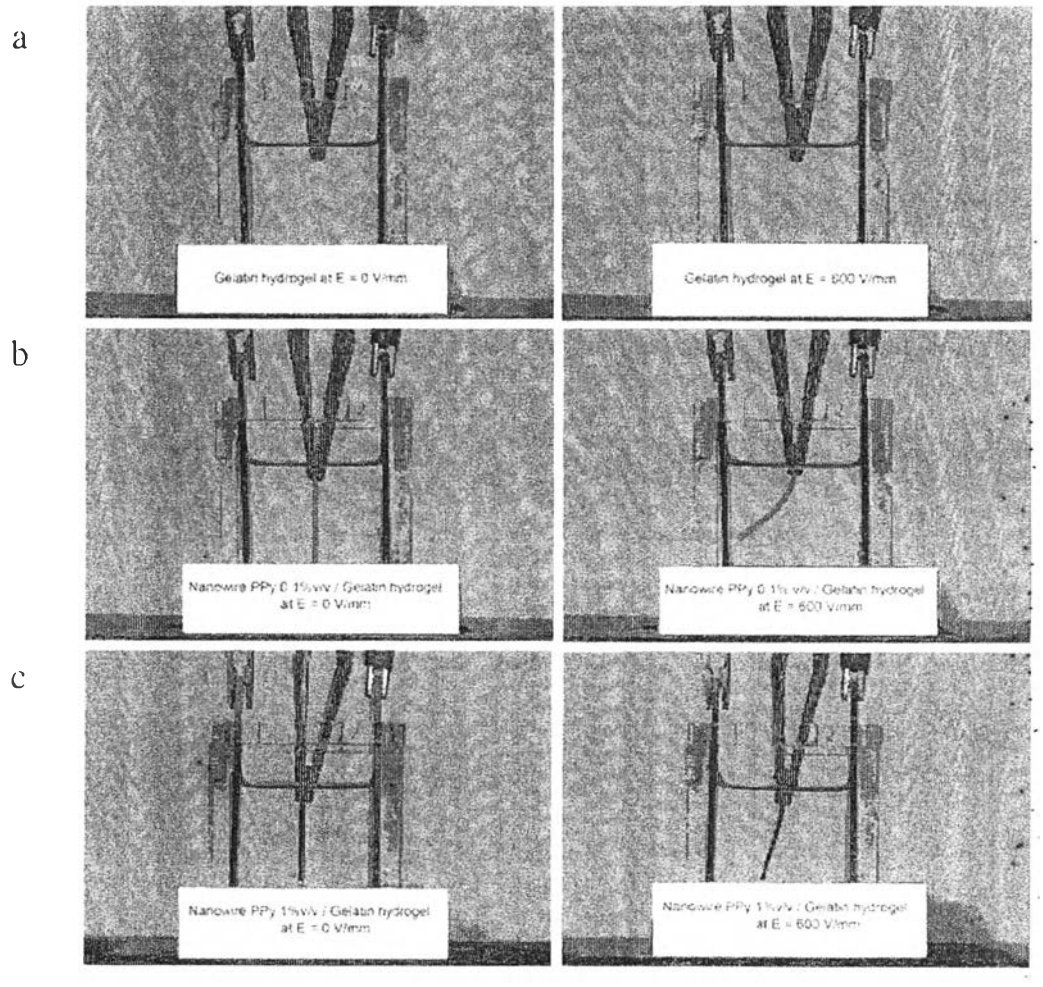

Figure 3.9 Deflection of the hydrogels at E = 0 and 600 V/mm: (a) pure gelatin hydrogel; (b) 0.1 %v/v nanowire Ppy/gelatin hydrogel; and (c) 1 %v/v nanowire Ppy/gelatin hydrogel. Note: The polarity of the electrode on the left hand side is positive.

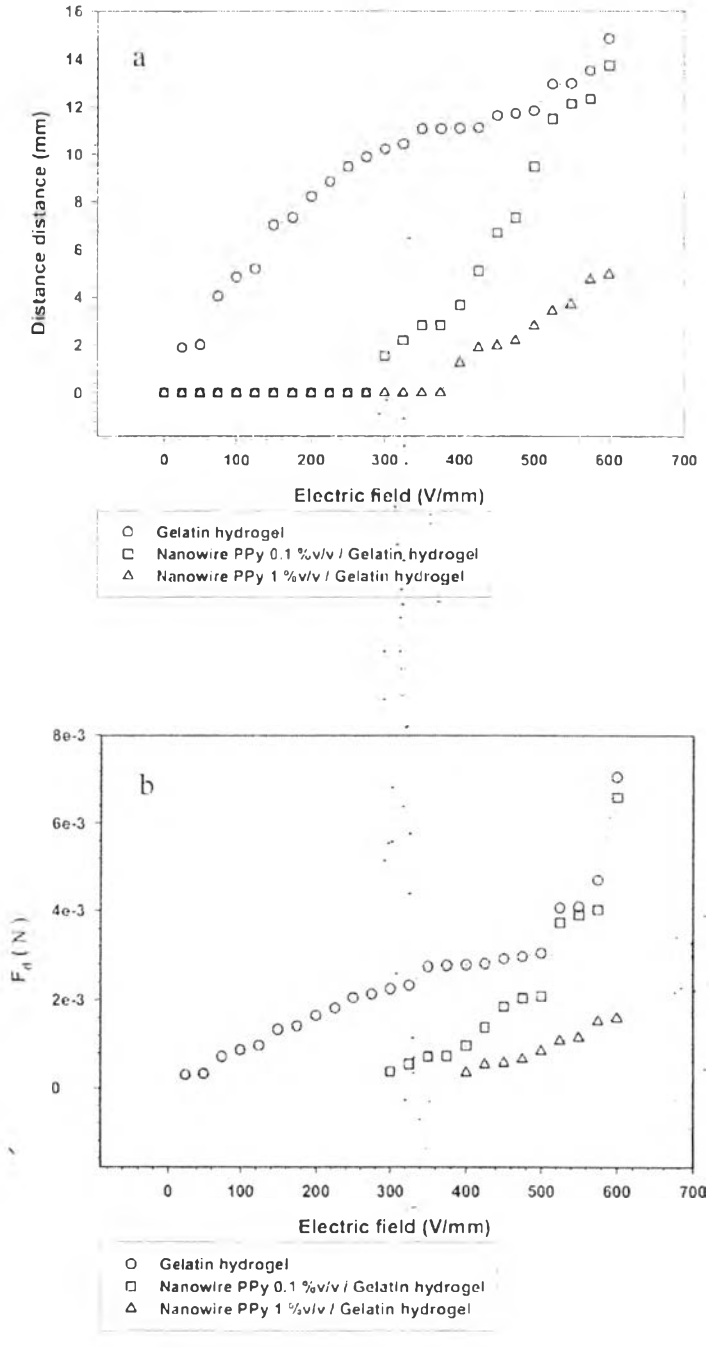

Figure 3.10 (a) Deflection distances of the gelatin hydrogel, the 0.1 %v/v nanowire Ppy/gelatin hydrogel, and the 1 %v/v nanowire Ppy/gelatin hydrogel at various electric field strengths and (b) Dielectrophoretic force calculated through the Linear Deflection theory.

Table 3.1 FTIR characteristic peaks of synthesized polypyrrole

Wavenumber (cm-1)	**Assignment**
1547, 1450	Pyrrole ring
1302, 1038	=C-H in plane
1178	C-N stretching
633	Sulfonate anion

Table 3.2 Avarage particle sizes and electrical conductivity data of the Ppy synsthesized at different DBSA/pyrrole ratios

Concentration of DBSA and pyrrole ratio (N_{DBSA}:$N_{monomer}$)	Avarage particle sizes (nm)	Conductivity (S/cm)
0.01:1	370 ± 28.10	0.76 ± 0.0002
0.1:1	250 ± 40.30	1.37 ± 0.0009
0.5:1	195 ± 14.20	2.30 ± 0.0023
1:1	95 ± 18.00	23.86 ± 0.032
5:1	53 ± 4.10	15.41 ± 0.018
10:1	49 ± 2.60	15.95 ± 0.011

Table 3.3 Sensitivity of the storage modulus of the pure gelatin and the Nanowire Ppy /gelatin hydrogels: 0.15 % strain, electric field strength 800 V/mm, frequency of 100 rad/s, and at 30 °C

Material (nanowire Ppy diameter: 95 ± 18 nm)	**Storage modulus (G') Pa**	**Initial storage modulus (G'_o) Pa**	**Sensitivity of storage modulus ($\Delta G'/G'_o$) Pa**
Gelatin hydrogel (Ge)	790 000	540 000	0.46
Ge – 0.01 % v/v nanowire Ppy	1 170 000	667 000	0.75
Ge – 0.1 % v/v nanowire Ppy	1 970 000	965 000	1.04
Ge – 0.5 % v/v nanowire Ppy	447 100	234 010	0.88
Ge – 1 % v/v nanowire Ppy	406180	203 401	0.99